한국지하수토양환경학회지 Vol. 9, No. 1, pp. 1~11, 2004 ≪原著≫

Foams for Aquifer Remediation: Two Flow Regimes and Its Implication to Diversion Process

Seung Ihl Kam[1] · Jonggeun Choe[2]*

[1]Australian School of Petroleum, The University of Adelaide, SA 5005 Australia
[2]Member, Research Institute of Engineering Science, School of Civil, Urban and Geosystems Engineering, Seoul National University

ABSTRACT

Foam reduces the mobility of gas phase in porous media to overcome gravity override and to divert acid into desired layers in the petroleum industry and to enhance the efficiency of environmental remediation. Recent experimental studies on foam show that foam exhibits a remarkably different flow rheology depending on the flow regime. This study, for the first time, focuses on the issues of foam diversion process under the conditions relevant to groundwater remediation, combining results from laboratory linear-flow experiments and a simple numerical model with permeability contrasts. Linear flow tests performed at two different permeabilities (k = 9.1 and 30.4 darcy) confirmed that two flow regimes of steady-state strong foams were also observed within the permeability range of shallow geological formations. Foam exhibited a shear-thinning behavior in a low-quality regime and near Newtonian rheology in a high-quality regime. Data taken from linear flow tests were incorporated into a simple numerical model to evaluate the efficiency of foam diversion process in the presence of permeability contrasts. The simple model illustrated that foam in the high-quality regime exhibited a successful diversion but foam in the low-quality regime resulted in anti-diversion, implying that only foam in the high-quality regime would be applicable to the diversion process. Sensitivity study proved that the success of diversion process using foam in the high-quality regime was primarily controlled by the limiting capillary pressures (P_c^*) of the two layers of interest. Limitations and implications are also discussed and included.

Key words : foam, diversion, remediation, groundwater, aquifer

요 약 문

다공성 매질내의 거품(foam)은 가스상의 이동성을 감소시키는 특성을 가진다. 이러한 성질은 석유산업에서 중력으로 인한 유체유동을 방지하거나 산(acid)을 이용하여 유정(wellbore) 근처 유체투과율이 낮은 지층을 처리하는데도 사용될 뿐만 아니라, 지하 대수층의 오염물 회수율을 높이는 데도 사용된다. 최근의 연구결과를 통하여 다공성 매질 내 거품의 유동은 유동영역(flow regime)에 의하여 크게 영향을 받는다는 사실을 규명하였다. 이 논문은 실험자료와 수치해석기법을 이용하여, 지하 오염물질 정화를 위한 거품 유동분할 작업의 타당성에 관한 연구이다. 두 종류의 유체투과율(k=9.1과 30.4 darcy)을 가지고 실험한 결과, 대수층 조건과 비슷한 실험환경에서도 정상상태의 거품은 유동영역에 따라 다른 성질을 보인다는 사실을 알 수 있었다. 거품의 질이 낮은 영역(low-quality regime)에 있는 거품은 shear thinning 거동을 보이며 고질영역(high-quality regime)에 있는 거품은 Newtonian 거동과 유사하였다. 이상의 실험 결과를 유체투과율이 서로 다른 두 지층에 대하여 거품의 유동분할을 예측하기 위하여 간단한 수치해석 모델을 개발하였다. 수치해석의 결과로부터 고질영역에 있는 거품은 유동분할 양상을 보였지만 저질영역에 있는 거품은 그렇지 않았다. 민감도 분석의 결과 고질영역에서의 유동분할은 각 지층들의 한계 모세관압, 즉 거품이 생성되고 유지되기 위한 최소 모세관압에 의해 좌우된다는 사실을 확인하였다.

주제어 : 거품, 유동분할, 오염토양정화, 지하수, 대수층

*Corresponding author : johnchoe@snu.ac.kr
원고접수일 : 2003. 04. 14 게재승인일 : 2003. 8. 19
질의 및 토의 : 2004. 6. 30 까지

1. Introduction

Foam is a versatile means in many applications in porous media. Foam has been extensively studied in connection with gas injection in improved oil recovery and acid diversion in well stimulation treatments in the petroleum industry[1-3]. Foam has also been proven to be effective in field-scale pilot tests of shallow groundwater remediation[4,5]. Foam is able to reduce gas mobility within porous media and thus greatly improve sweep efficiency. Because of the interplay between foam stability and capillary pressure, foam is believed to even-out flow in the presence of permeability contrasts or the heterogeneity of geological formations. Complex nature of foam in diversion process and its limitations, however, are not fully understood.

Foam in porous media can be defined as a dispersion of gas phase in liquid phase (i.e., surfactant solution) such that the liquid phase is continuous and connected and at least some gas paths are blocked by thin liquid films, called lamellae.[2,6,7] The ability of foam to reduce gas mobility depends strongly on its texture, i.e., bubble size or the number of lamellae per unit volume. It is the foam texture that decides the degree of reduction in gas mobility during foam flow in porous media. Foam texture, in fact, is a result of two dynamic events such as lamella generation and coalescence. The two events are sensitive to many factors such as properties of fluids and porous media, injection rates and methods, surfactant formulations and concentrations, surrounding temperature and pressures, and many others.

Foam generation represents a sudden drastic change from a state of high gas mobility with a small number of lamellae per unit volume (i.e., coarse foam texture) to a state of low gas mobility with a large number of lamellae per unit volume (i.e., fine foam texture)[1,2,6]. Foam generation is a process where the rate of lamellae creation greatly exceeds the rate of lamellae destruction. The onset of foam generation is often observed with a dramatic increase in the pressure gradient in lab-scale flow experiments. Among many, Gauglitz *et al.*[8] conduct their experiments at fixed pressure as well as fixed rates. They find that the process of foam generation can be described by a smooth, 3D surface of pressure gradient as a function of injection rates and the surface folds back and forth from weak foam to transient foam, and finally to strong foam. They reveal that the abrupt increase in the pressure gradient, often called the minimum pressure gradient for foam generation (∇P^{min}), is inevitable in fixed-rate foam generation experiments. An existing population-balance model combined with the lamella division and mobilization as main mechanism in porous media is able to predict the same trends at a steady state[9].

Osterloh and Jante,[10] for the first time, show that there exist two steady-state foam flow regimes in 2-ft (60.96 cm) sandpack experiments once strong foam is attained in porous media. Alvarez *et al.*[11] further explore and observe that two steady-state strong-foam regimes exist consistently in a variety of different surfactant formulations and permeabilities for the use of foam in the petroleum industry. Others also observe the same trends in their laboratory experiments in connection with groundwater remediation in shallow subsurface[12] and foam-acid diversion processes at elevated temperature in the presence of acid[13]. Mamun et al.[14], based on their experimental data, prove that foam can sweep a shallow subsurface provided that the minimum pressure gradient for foam generation can be scaled down to a pressure gradient relevant to aquifer remediation, which is in fact contradictory to the theory of foam generation in porous media in a degree[2,8,15].

Studies on foam diversion processes for shallow groundwater remediation require consistent data sets. Data in high-permeability media are lacking and existing data do not provide valuable insights because of different experimental conditions applied. This study is devoted to measure rheological characteristics of steady-state strong foams at two different permeabilities under the conditions relevant to aquifer remediation. Data interpretation from the experimental results, combined with a simple model with two geological layers differing permeability, presents applicability and limitation of foam as a diversion agent to overcome the heterogeneity of shallow subsurface.

The complex nature of diversion process within multiple layers with different values of permeability, the crossflow across the layers in capillary contact and its mathematical description, and the effect of contaminants on lamellae stability and foam rheology are, however, beyond the scope of this study. Also, this study narrows its scope to fine-textured strong foams, not dealing with complex nature of foam generation in porous media.

2. Theory

Many studies find that foam exhibits two distinct flow behaviors depending on injected gas volume fraction, i.e., foam quality (f_g), once strong foam is created. Fig. 1 illustrates one example from the study of Osterloh and Jante[10] with steady-state pressure gradients during foam flow expressed in contours with the volumetic liquid flux in x axis and the volumetric gas flux in y axis. The experiments were conducted at elevated back pressure of 200 psia (1379 kPa) and temperature of 302°F (150°C) with a mixture of 0.25 wt.% of a linear C16-18 a-olefin sulfonate and 0.25

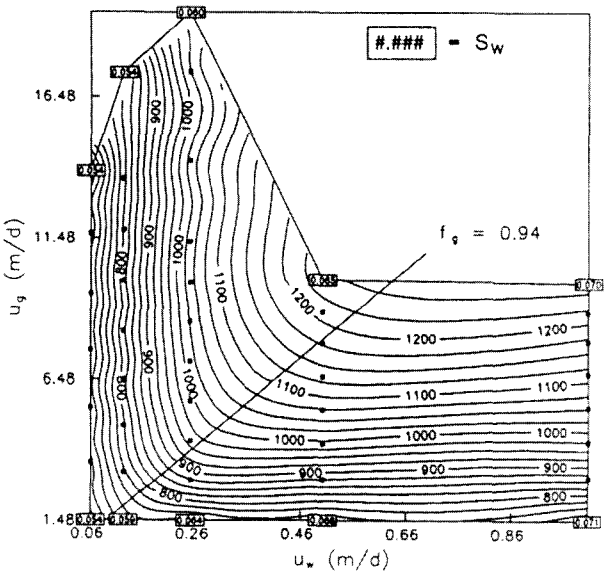

Fig. 1. Contours of steady-state pressure drop across a 2-ft sandpack from Osterloh and Jante [10] illustrating two strong-foam regimes. The pressure values along the contours are in units of psi (1 psi = 6900 Pa).

wt.% of a linear C16 diphenyloxide disulfonate. Total pressure drop across 2 ft pack is specified along the pressure contours in a unit of psi and a steady-state average water saturation is shown by boxed numbers in Fig. 1. In the high-quality regime (upper-left portion of Fig. 1), the pressure-gradient contours are nearly vertical meaning that the pressure gradient is almost independent of gas velocity (U_g). In this regime, foam rheology is primarily governed by bubble coalescence at a fixed value of capillary pressure, so-called "the limiting capillary pressure (P_c^*)",[16-18] and therefore foam texture changes significantly with gas velocity.[11] Because capillary pressure is related to water saturation in porous media, there exists a value of water saturation (S_w), i.e, S_w^*, corresponding to P_c^*. Therefore, based on the fact that the liquid relative-permeability function is not affected by the presence of foam,[1,2,19,20] Darcys equation for gas and liquid can be written as

$$U_g=\frac{kk_{rg}^f(S_w^*)}{\mu_g^f}\nabla P=k\lambda_{rg}^f(S_w^*)\nabla P=\frac{kk_{rg}^f(S_w^*)}{\mu_g MRF}\nabla P \quad (1)$$

and

$$U_W=\frac{kk_{rw}(S_w^*)}{\mu_w}\nabla P=k\lambda_{rw}^f(S_w^*) \quad (2)$$

where U_g and U_w represent Darcys velocities of gas and liquid phases (i.e., gas and liquid volumetric fluxes), ∇P pressure gradient, k absolute permeability, k_{rj} the relative permeability of phase j, μ_j the viscosity of phase j, MRF the mobility reduction factor of gas phase by the presence of foam, and λ_{rj} the relative mobility of phase j. Subscripts g and w represent gas and water phases, respectively, and superscript f the presence of foam.

The presence of lamellae in porous media influences both gas relative-permeability function and gas viscosity. Because there is no clear cut to separate these two effects, it is often convenient to put these effects into a single term, either gas relative mobility (λ_{rg}^f) or mobility reduction factor (MRF) of gas phase as in Eq. (1). Darcys equation for liquid phase (Eq. (2)) implies that once water relative-permeability function is known or properly estimated, one can calculate S_w^* from the data set of pressure measurements and liquid rates.

If the theory of the limiting capillary pressure is perfect, it implies that the pressure-gradient contours are nearly vertical and foam exhibits Newtonian rheology in the high-quality regime. Also because ∇P is independent of U_g from Eq. (1), one can infer that bubble size becomes bigger (i.e., foam texture becomes coarser) as U_g increases at a fixed U_w[9,11]. Put it differently, the increase in U_g in the high-quality regime is compensated by the reduction in gas viscosity, which results from the coarsening of foam texture.

In the low-quality regime (lower-right portion of Fig. 1), the pressure gradient is nearly independent of liquid rate. Because the bubble size in this regime is thought to be fixed and almost the same as pore size, foam rheology is controlled by bubble trapping and mobilization resulting in a highly shear-thinning rheology. Cheng *et al.*[21] applied the same concept to simulate the diversion process of acids following foam during post-foam liquid injection stage to improve hydrocarbon recovery from the petroleum reservoir. Darcys equation is also applicable to describe foam rheology, i.e.,

$$U_w=\frac{kk_{rw}(S_w)}{\mu_w}\nabla P=k\lambda_{rw}(S_w)\nabla P \quad (3)$$

and

$$U_g=\frac{kk_{rg}^f(S_w)}{\mu_g^f}\nabla P=k\lambda_{rg}^f(S_w)\nabla P=\frac{kk_{rg}^f(S_w)}{\mu_g MRF}\nabla P. \quad (4)$$

Note that the water saturation is no longer hinged at S_w^* in the low-quality regime.

The fact that ∇P is independent of U_w from Eq. (3) suggests that water saturation changes to compensate the change in liquid injection rate. In other words, increasing U_w results in the invasion of liquid into the bigger pores mobilizing part of trapped bubbles.[11,22] Measurement of foam viscosity in capillary tubes shows the dependence of $\mu_g \sim (1/U_g)^{2/3}$[23]. If there is viscosity effect alone without relative permeability effect, this implies that a shear-thinning exponent of foam rheology in the low-quality regime would be around 2/3. Because water saturation decreases with U_g, combining the effects of gas viscosity and gas relative permeability would reduce the shear-thinning exponent even less than 2/3. The

shear-thinning behavior can be expressed in general by

$$\frac{\nabla P}{\nabla P^{ref}}=\left(\frac{U_g}{U_g^{ref}}\right)^n \quad (5)$$

where n is a shear-thinning exponent and ∇P^{ref} and U_g^{ref} represent a pressure gradient and gas volumetric flux measured at an arbitrary reference datum, respectively. Eq. (5) implies that once the shear-thinning exponent is known, one may predict foam rheology in the low-quality regime without dealing with detailed descriptions on foam texture. In other words, complex nature of bubble trapping and mobilization in the low-quality regime can be bypassed by a simple expression of the shear-thinning rheology as long as foam in porous media reaches a steady state instantaneously[21,22]. The two flow regimes are separated by a value of foam quality, f_g^*, which is found to be affected by many factors including permeability, surfactant formulations, and surfactant concentration[11,12].

3. Experiment and Discussion

3.1. Experimental Procedure

Linear flow experiments were conducted to measure foam rheology in porous media. Fig. 2 shows a schematic of the apparatus. Liquid was injected by a syringe pump and gas phase was regulated by a mass flow meter. The liquid phase was 0.5 wt % of sodium α-olefin sulfonate added into the brine solution, 1 wt% NaCl in deionized water, and the gas phase was nitrogen in all experiments.

A specially designed packholder, 12-inch (30.48 cm) long and 1.1-inch (2.79 cm) in inner diameter with three pressure taps along its side, was used to observe sectional pressure gradients using differential pressure transducers and these transducers allowed one to estimate the location of foam front in the pack. The four sections were 2.37, 3.63, 3.63, and 2.37-inch long from the inlet of the packholder that was mounted in a vertical direction with fluid injection from the top throughout the experiments.

A filter with 2-μm opening size was installed upstream of the packholder to pre-generate foams and a visual cell confirmed the generation of fine-textured foam before foam enters the pack. The other visual cell installed at the outlet provided indirect indication on how foam texture changed at different injection conditions. A backpressure regulator maintained the pressure at the outlet of the apparatus at 100 psi (690 kPa) in all experiments. The packholder was filled with either silica sands or glass beads of nominal diameter 100 μm. Both sands and beads were believed to be of uniform sizes and shapes. For a uniform packing, the sands and beads were added to the packholder continuously over a period of 40 or 50 minutes with the pack vibrated gently. Permeability (k) was around 9.1 and 30.4 darcy for sandpack and beadpack respectively, and the porosity (ϕ) was about 0.31 in both cases. These permeability and porosity values are taken for numerical calculation to evaluate diversion capability of foams in two non-communicating layers.

3.2 Experimental Results

Fig. 3 shows the results of beadpack experiment (k= 30.4 darcy). Black dots represent steady-state pressure gradients and dashed curves delineate the trend of the data. Two flow regimes are observed as in other studies [9-12] and f_g^* ranges around 90-93%. Fig. 4 illustrates foam rheology

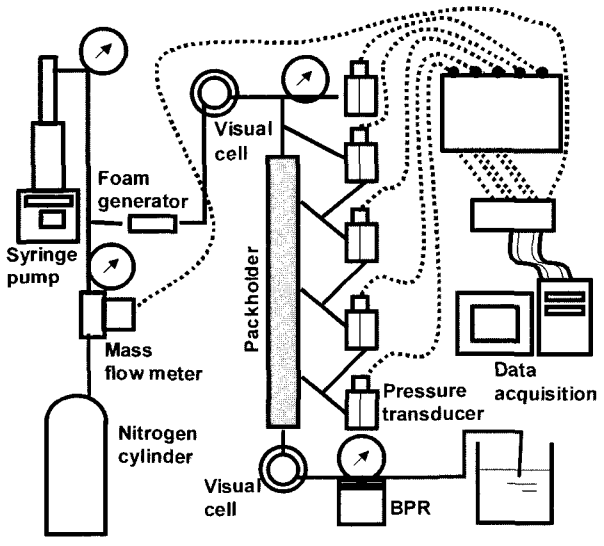

Fig. 2. Schematic of laboratory linear flow apparatus.

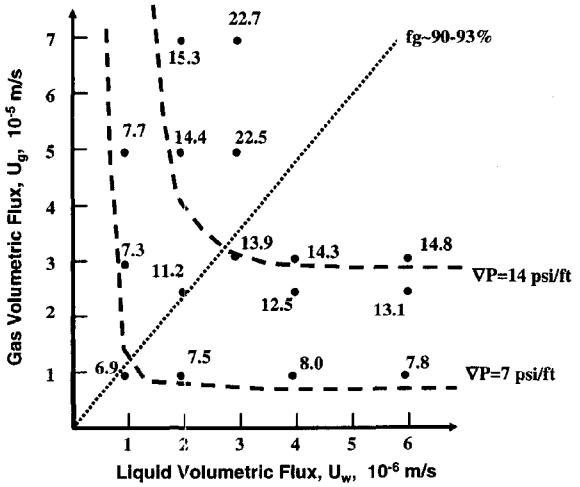

Fig. 3. Two steady-state strong-foam regimes using a beadpack with k= 30.4 darcy and ϕ= 0.31. Separation between the high- and low-quality regime occurs near f_g^*=90-93%. The pressure-gradient values reported are in units of psi/ft (1 psi/ft = 22626 Pa/m).

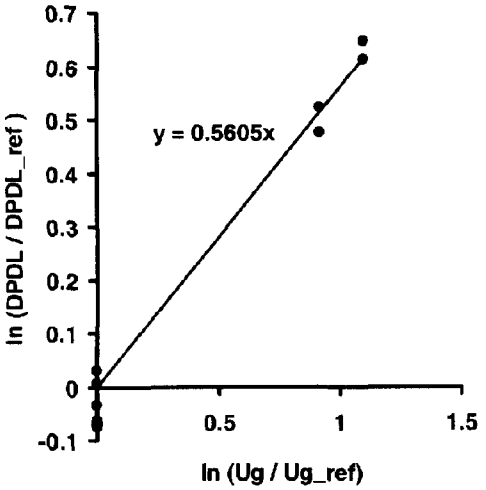

(a) Low-quality regime

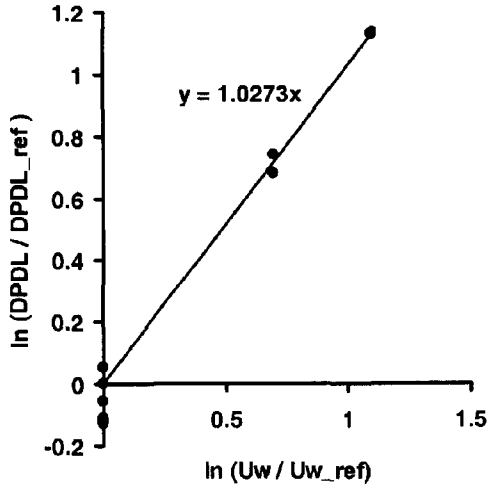

(b) high-quality regime

Fig. 4. Determination of the power-law exponent (the slope) of foam in 30.4-darcy beadpack.

in two flow regimes demonstrating detailed calculations of a power-law exponent (n). A shear-thickening rheology has n > 1 and a shear-thinning rheology has n < 1. The value of n close to 1 means near Newtonian behavior. As denoted in Eq. (5), the power-law exponent is the slope of a log-log plot of pressure gradient vs. injection rate, i.e.,

$$\ln\left(\frac{\nabla P}{\nabla P^{ref}}\right)=n\ln\left(\frac{U_w}{U_w^{ref}}\right) \text{ or } \ln\left(\frac{\nabla P}{\nabla P^{ref}}\right)=n\ln\left(\frac{U_g}{U_g^{ref}}\right) \quad (6)$$

for the high- and low-quality regimes, respectively. Curve fitting shows the exponents close to 1.03 in the high-quality regime and 0.56 in the low-quality regime. Therefore, foam rheology is near Newtonian behavior (i.e., n~1) in the high-quality regime, enabling one to use Eqs. (1) and (2) to analyse flow behavior. Highly shear-thinning behavior in the low-

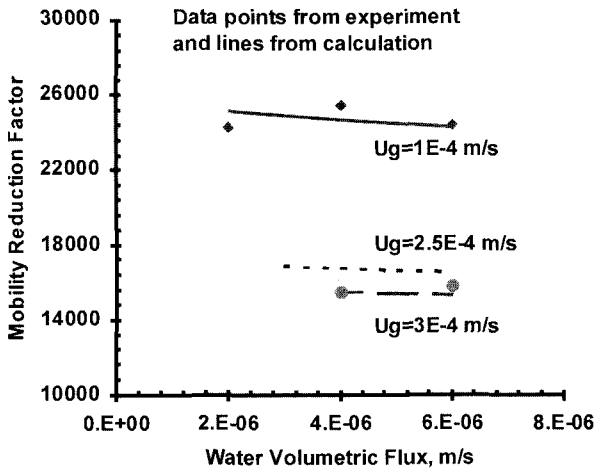

Fig. 5. Comparing mobility reduction factor (MRF) of foam in the low-quality regime (experimental data vs. model prediction using a power-law exponent) for 30.4-darcy beadpack.

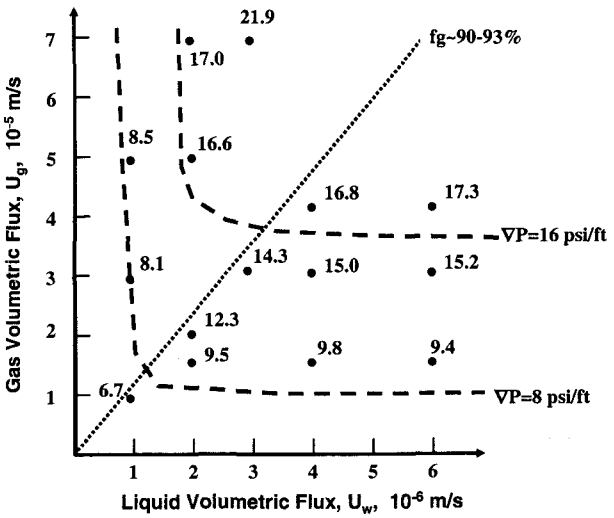

Fig. 6. Two steady-state strong-foam regimes using a sandpack with k= 9.1 darcy and ϕ= 0.31. (f_g^*=90-93%). The pressure-gradient values reported are in units of psi/ft (1 psi/ft = 22626 Pa/m).

quality regime is also consistent with previous experimental studies at high surrounding pressures[10,11].

A comparison is made to ensure how simple description with a shear-thinning parameter as in Eq. (5) fits the trend of foam in the low-quality regime as in Fig. 5. Mobility reduction factor (MRF) in Eq. (2) is selected by a means of verification, putting the effect of gas relative permeability and gas viscosity together. Data points are taken from the low-quality regime of the contour plot (Fig. 3) and lines are the trend predicted by Eqs. (5) and (6). Two results are in good agreement. It is not clear at this stage, however, whether this approximation using a shear-thinning parameter would be consistent beyond the range investigated in this study.

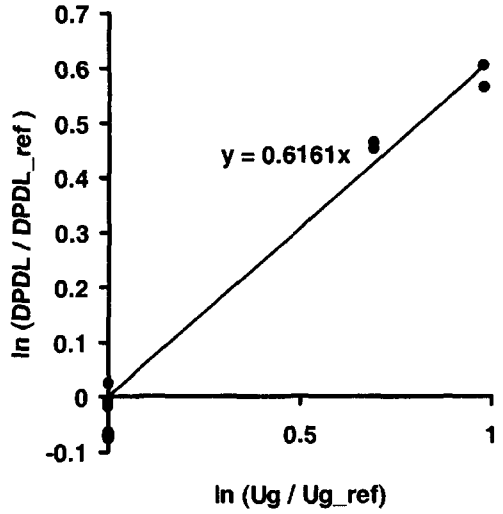

(a) Low-quality regime

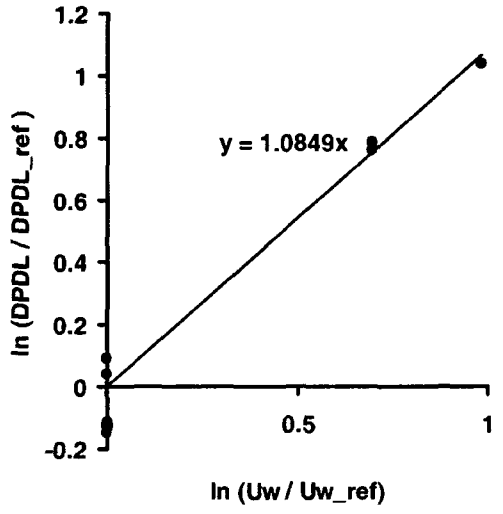

(b) high-quality regime

Fig. 7. Determination of the power-law exponent (the slope) of foam in 9.1-darcy sandpack.

Fig. 6 shows a steady-state pressure-gradient contour of sandpack experiment (k= 9.1 darcy). Two flow regimes are also observed at a different value of permeability and f_g^* ranges around 90-93%. The power-law exponents calculated from the experimental data, as shown in Fig. 7, are about 1.08 and 0.616 for the high-, and low-quality regimes, respectively. The tendency of near Newtonian rheology in the high-quality regime and highly shear-thinning rheology in the low-quality regime is observed consistently. Fig. 8 shows good agreement in MRF between the experiments and the calculations.

3.3 Foam Diversion

The two contour plots at different permeabilities make it possible to evaluate the effectiveness of diversion processes using foam. Fig. 9 shows a schematic of an example problem to be solved to test foam diversion processes, i.e., two layers with different permeabilities isolated by an impermeable boundary in between. Note that the two permeabilities (9.1 and 30.4 darcy) and the porosity of 0.31 in both layers are given by the linear flow experiments. Both layers are saturated with water (S_w=1) initially and are of equal length and thickness. Foam at a specific foam quality is injected at fixed rates and the pressure at the outlet is kept constant and identical. Therefore, total pressure drop (ΔP_t) in each layer is simply the sum of pressure drops in a zone with foam (ΔP_{foam}) and zone with water (ΔP_{water}), i.e.,

$$\Delta P_{t,1}=\Delta P_{foam,1}+\Delta P_{water,1}=(\nabla P_{foam,1})L_1+(\nabla P_{water})(L_t-L_1) \quad (7)$$

for layer 1 with a high permeability (k= 30.4 darcy) and

$$\Delta P_{t,2}=\Delta P_{foam,2}+\Delta P_{water,2}=(\nabla P_{foam,2})L_2+(\nabla P_{water,2})(L_t-L_2) \quad (8)$$

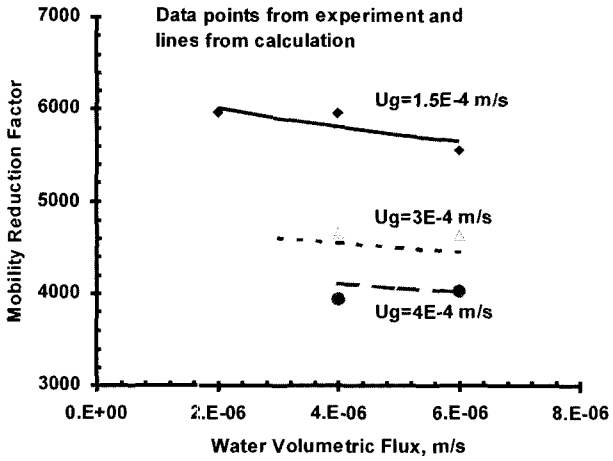

Fig. 8. Comparing the mobility reduction factor (MRF) of foam in the low-quality regime (experimental data vs. model prediction using a power-law exponent) for 9.1-darcy sandpack.

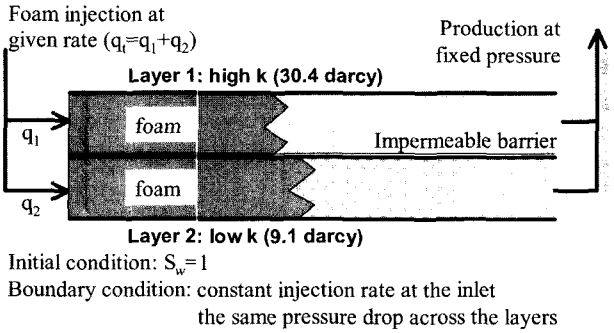

Fig. 9. Schematic of a simple model for diversion calculations.

for layer 2 with a low permeability (k = 9.1 darcy), where L_t is the total length of the layers and L_1, L_2 the positions of foam front from the inlet in layer 1 and 2 respectively. Subscripts 1 and 2 represent layer 1 and 2, respectively. Eqs. (7) and (8) imply that the position of foam front in each layer is primarily determined by foam rheology at each layer. It is further assumed that gas and liquid are incompressible. Finite difference method was applied to solve Eqs. (7) and (8), together with Darcys equations (Eqs. (1) through (4)) and two other conditions such as;

$$\Delta P_{t,1}=\Delta P_{t,2} \tag{9}$$

and

$$q_t=q_1+q_2 \tag{10}$$

Eq. (9) states that the two layers, though not communicating, have the same pressure drop and Eq. (10) the material balance.

Substituting Darcys law into Eq. (7), for layer 1, leads to

$$\Delta P_{t,1}=\left(\frac{U_{g,1}}{k_1 k^f_{rg,1}(S_w)/\mu^f_{g,1}}+\frac{U_{g,1}}{k_1 k_{rw,1}(S_w)/\mu_w}\right)L_1 + \left(\frac{U_{g,1}+U_{w,1}}{k_1/\mu_w}\right)(L_t-L_1) \tag{11}$$

Since the pressure gradient is independent of gas flow rate in the high-quality regime, Eq. (11) further simplifies to

$$\Delta P_{t,1}=\left(\frac{U_{w,1}}{k_1 k_{rw,1}(S_{w,1}{}^*)/\mu_w}\right)L_1+\left(\frac{U_{g,1}+U_{w,1}}{k_1/\mu_w}\right)(L_t-L_1) \tag{12}$$

Likewise, the equation for foam in the low-quality regime becomes

$$\Delta P_{t,1}=\left(\frac{U_{g,1}}{U_{g,1}}\right)^n \nabla P_1^{ref} L_1+\left(\frac{U_{g,1}+U_{w,1}}{k_1/\mu_w}\right)(L_t-L_1) \tag{13}$$

Therefore, the intake of foam in each layer is controlled primarily by permeability and $S_w{}^*$ in the high-quality regime and by permeability and the power-law exponent in the low-quality regime.

The transition zone between the two flow regimes near $f_g{}^*$, which is beyond the scope of this study, is more complicated and therefore should follow the expression as in Eq. (11). It should be noted that the simplification made for the high- and low-quality foams would predict better results as the contours become more vertical and more horizontal in the high- and low-quality regimes, respectively. Therefore, this simplification using Eqs. (11) and (12) is not applicable to the foams near $f_g{}^*$ where the contours significantly deviate from the either of the trend.

3.3.1. Diversion in the high-quality regime

The vertical pressure-gradient contours imply that foam rheology can be explained by the limiting capillary pressure[16-18] as explained in Eqs. (1) and (2). The relative-permeability functions for water and gas are assumed to be identical to those measured in the similar sandpack and beadpack experiments[24], i.e.,

$$k_{rw}=0.7888\left(\frac{S_w-S_{wc}}{1-S_w-S_{gr}}\right)^{1.9575} \tag{14}$$

and

$$k_{rg}=\left(\frac{1-S_w-S_{gr}}{1-S_{wc}-S_{gr}}\right)^{2.2868} \tag{15}$$

Parameter values selected in the calculations are: connate water saturation (S_{wc}) = 0.04, residual gas saturation (S_{gr}) = 0, liquid viscosity (μ_w) = 1 cp and gas viscosity (μ_g) = 0.02 cp.

Eqs. (1), (2), (14) and (15) allow one to calculate $S_w{}^*$ and the result is shown in Figure 10. The symbols represent calculated $S_w{}^*$ from the experimental data shown in Figs. 3 and 6. As expected by the theory of the limiting capillary pressure, the data clearly show that $S_w{}^*$ is almost constant in the high-quality regime with the values of 0.054 and 0.065 for the high- and low-permeability layers, respectively.

Fig. 11 shows the fraction of foam into each layer using the values of $S_w{}^*$ taken from Fig. 10. Initially, due to the permeability contrast, the high-permeability layer (layer 1) takes about 77% of the total injected foams and the low-permeability layer (layer 2) takes the rest 23%. Then foam diversion takes place immediately as foam propagates into the layers. Note that it is the limiting capillary pressure, $P_c{}^*$, (or $S_w{}^*$ equivalently) that results in the success of diversion process. In other words, main cause of foam diversion is that the foam strength, or MRF (*c.f.*, Eq(1)) equivalently, becomes higher in the high-permeability layer due to the difference in $S_w{}^*$ in the layers. During the steady

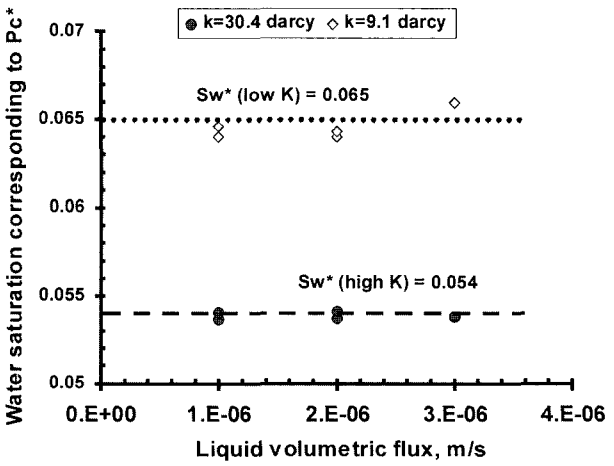

Fig. 10. Calculation of $S_w{}^*$ from experimental results. $S_w{}^*$ is almost constant for foam in the high-quality regime.

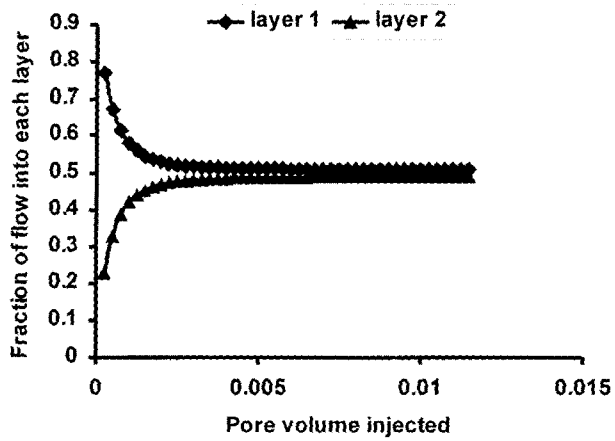

Fig. 11. Diversion of foam in the high-quality regime. Diversion greatly improves the flow of foam into the low-permeability layer from 23 to 49%.

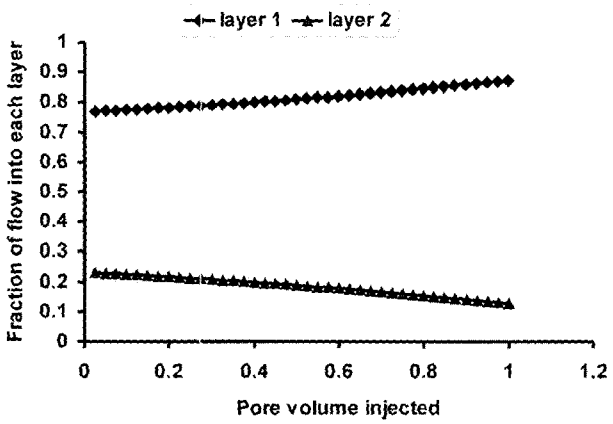

Fig. 12. Anti-diversion of foam in the low-quality regime. More fluid flows into the high-permeability layer.

state achieved after about 0.01 pore volume (PV) injection, the high- and low-permeability layers admit 51% and 49% of the injected fluid.

3.3.2. Diversion in the low-quality regime

Fig. 12 shows the results of diversion processes using foam in the low-quality regime. Rheological properties of foam in this regime are taken from the results of shear-thinning exponents (Eq. (5), and Figs. 5 and 8), i.e., the power-law exponents of 0.5605 for the high-permeability layer and 0.6161 for the low-permeability layer. Initially, the high-permeability layer (layer 1) takes about 77% of the total injected foams and the low-permeability layer (layer 2) takes 23%. But as foam continues entering the layers, the high-permeability layer takes more fluids and the low-permeability layer less fluids. This is the case of anti-diversion, diverting more flow into the high-permeability layer than the low- permeability layer without gaining any advantages of using foam.

3.3.3. Sensitivity study

Because Figs. 11 and 12 show a drastic difference in the ability of foam in diversion processes, further tests are performed to check the sensitivity of the results. Fig. 13 shows two example calculations for foam in the high-quality regime; Fig. 13(a) with the increase of S_w^* in the low-permeability layer (S_{w2}^*) from 0.065 to 0.08, keeping S_w^* in the high-permeability layer (S_{w1}^*) constant and Fig. 13(b) with the reduction in S_{w1}^* and S_{w2}^*, keeping the ratio

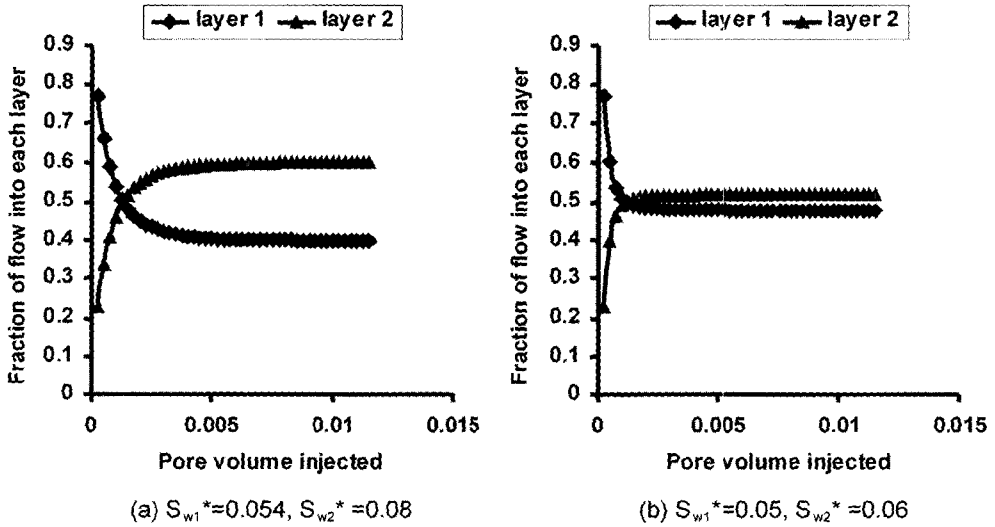

Fig. 13. Example of sensitivity check for foam in the high-quality regime. Base case (Figs. 10 and 11): S_{w1}^*=0.054, S_{w2}^*=0.065. (a) change of S_w^* in the low-permeability layer (S_{w2}^*) with S_w^* in the high-permeability layer (S_{w1}^*) fixed, (b) change of S_{w1}^* and S_{w2}^* with the ratio (S_{w2}^*/S_{w1}^*) fixed.

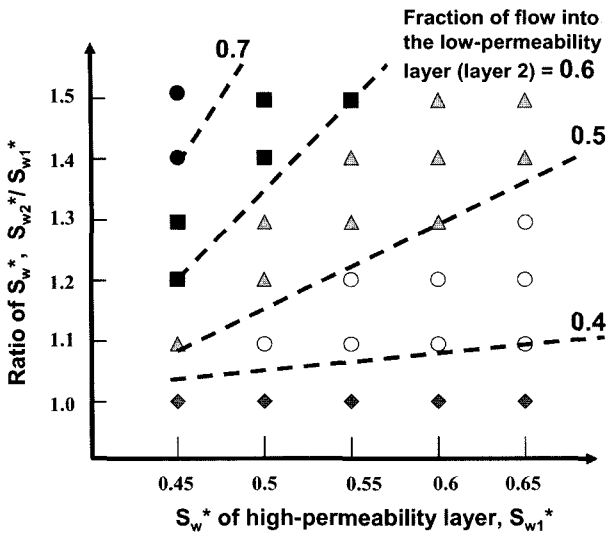

Fig. 14. Sensitivity of diversion process using foam in the high-quality regime as a function of S_{w1}^* and S_{w2}^*/S_{w1}^*. The contour values greater than 0.5 represents successful foam diversion resulting in more flow into the low-permeability layer.

(S_{w2}^*/S_{w1}^*) constant as in Fig. 11. Note that $S_{w1}^* = 0.054$ and $S_{w2}^* = 0.065$ from experiments (Fig. 10). In both cases, the efficiency of diversion process is improved significantly resulting in complete diversion, i.e., the low-permeability layer admits more flow. This implies that the diversion process in the high-quality regime is quite sensitive to S_{w1}^* and S_{w2}^*.

Fig. 14 demonstrates the sensitivity of diversion process of foam in the high-quality regime in terms of the fraction of flow into the low-permeability layer. Tests are performed for $S_{w2}^* = S_{w1}^*$ (the y-axis in Fig. 14) because S_{w1}^* can not be higher than S_{w2}^* based on the fact that P_c^* is not affected by permeability significantly. The fraction 0.5 represents the case that both high- and low-permeability layers intake equal amount of foam and the fraction greater than 0.5 means that the low-permeability layer intakes more flow. Also it should be noted that the fraction of 0.23 (i.e., 23% of fluid flowing into the low-permeability layer) is the value if there is no diversion effect. Results show that foam in the high-quality regime always helps diversion processes to some extent irrespective of S_{w1}^* and S_{w2}^*. The diversion process becomes more effective as S_w^* of the high-permeability layer (S_{w1}^*) decreases and the ratio of S_{w2}^*/S_{w1}^* increases. This implies that the diversion process is improved as foam in the high-permeability layer becomes stronger and the foam in the low-permeability layer becomes weaker.

Further sensitivity study on foam in the low-quality regime shows that the diversion process is insensitive to parameter change for the wide range of shear-thinning exponents as long as the exponents are less than 2/3.

3.4. Discussion

Experimental results, combined with a simple numerical model, show that the diversion of foam flow into the less-permeable layer happens only in the high-quality regime in which foam rheology is very sensitive to P_c^* and S_w^*. Data for P_c^* of foams in the high-quality regime are lacking, however. Because P_c^* and S_w^* are functions of surfactant formulations, surfactant concentration, petrophysical properties of porous media, temperature, and many others, the issue of measuring P_c^* and S_w^* deserves further studies to quantify the dependence of lamellae stability on permeability.

Indirect measurement of foam texture using a visual cell at the downstream of the packholder shows that bubble size becomes bigger with decreasing gas flow rate along the vertical pressure contour lines in the high-quality regime and bubble size almost invariant in the low-quality regime, which is in agreement with the previous experimental findings and numerical calculations[9,11,21,22].

The result of this study that foams in the high-quality regime are able to divert following foams into the low-permeability layer seems consistent with the previous experimental studies implying that the diversion process is more favorable with higher foam quality[25,26]. But it should be kept in mind that none of the existing studies can be compared with this study directly because of different surrounding pressure, inconsistent injection methodology, and the lack of data to infer the location of f_g^* that separates two flow regimes.

It is recognized that most petroleum oils tend to destabilize foam, reducing P_c^* of foams in porous media significantly. On the other hands, there are other contaminants such as chlorinated or fluorinated oils that are not believed to affect foam stability. Foam rheology in the presence of different contaminants, therefore, should be investigated prior to applying the diversion technique and a field-scale modelling of foam injection for groundwater remediation.

Effect of capillary crossflow between the layers with permeability contrasts is also important in the diversion process. Two competing mechanisms play important roles. (1) Because the diversion process of foam in the high-quality regime is sensitive to water saturation, even a small change in water saturation across the boundary of two layers can impact the efficiency of the processes remarkably. (2) On the other hand, given the fact that the well spacing in the subsurface remediation is not far (normally < 30 ft) and capillary crossflow is a slow mechanism compared to the convection of remediating fluid, capillary crossflow may not affect the foam diversion process significantly. This topic addresses further study.

4. Conclusions

Linear flow experiments were carried out to investigate the rheological properties of foam in porous media under the experimental conditions relevant to shallow subsurface remediation. The data taken from linear flow tests were incorporated into a simple numerical model to evaluate the ability of foam as a diversion agent.

1. Two-flow regimes of steady-state strong foams were observed consistently at two different permeabilities (k = 9.1 and 30.4 darcy). Foam quality that separates the two flow regimes, f_g^*, were within the range of 90-93% in both cases.

2. Both contour plots at the two different permeabilities showed that foam had near Newtonian rheology in the high-quality regime (the power-law exponent~1) and highly shear-thinning rheology in the low-quality regime (the power-law exponent < 2/3).

3. A simple model in the presence of permeability contrasts without crossflow proved that foam diversion process was significantly affected by the flow regime. Foam in the high-quality regime favored the diversion process, but foam in the low quality regime resulted in anti-diversion. This suggests that field remediation treatment using foam as a diversion agent should be designed at a relatively high foam quality and, if possible, be ensured that foams are in the high-quality regime.

4. Sensitivity study of foam in the high-quality regime showed that the diversion process became more effective as S_w^* of high-permeability layer (S_{w1}^*) decreased and the ratio of S_w^*, i.e., S_{w2}^*/S_{w1}^*, increased.

Acknowledgement

This work was supported by the Small Research Grants Scheme by the University of Adelaide, Australia.

References

1. Schramm, L.L. (ed.), Foams: Fundamentals and Applications in the Petroleum Industry, ACS Advances in Chemistry Series No. 242, Am. Chem. Soc., Washington, DC (1994).
2. Rossen, W.R., Foams in Enhanced Oil Recovery, in Foams: Theory, Measurements and Applications, R.K. Prud'homme and S. Khan (eds.). Marcel Dekker, New York (1996).
3. Lake, L., Enhanced Oil Recovery, Prentice Hall, Eaglewood Cliffs, NJ (1989).
4. Hirasaki, G.J., Jackson, R.E., Jin, M., Lawson, J.B., Londergan, J., Meinardus, H., Miller, C.A., Pope, G.A., Szafranski, R., and Tanzil, D., "Field Demonstration of the Surfactant/Foam Process for Remediation of a Heterogeneous Aquifer Contaminated with DNAPL," in NAPL Removal: Surfactants, Foams, and Microemulsions, S. Fiorenza, C.A. Miller, C.L. Oubre, and C.H. Ward, (eds.), Lewis Publishers, Boca Raton (2000).
5. Hirasaki, G.J., Miller, C.A., Szafranski, R., Lawson, J.B., and Akiya, N. "Surfactant/Foam Process for Aquifer Remediation," *paper SPE 37257 presented at the SPE international Symposium on Oil Field Chemistry, Houston, TX, 18-21 Feb.* (1997).
6. Friedmann, F. and Jensen, J.A. "Some Parameters Influencing the Formation and Propagation of Foams in Porous Media," *paper SPE 15087 presented at the SPE California Regional Meeting, Oakland, CA, 2-4 April* (1986).
7. Falls, A.H., Hirasaki, G.J., Patzek, T.W., Gauglitz, P.A., Miller, D.D., and Ratulowski, J., "Development of a Mechanistic Foam Simulator: The Population Balance and Generation by Snap-Off," *SPERE*, pp. 884-892 (Aug. 1988).
8. Gauglitz, P.A., Friedmann, F., Kam, S.I., and Rossen, W.R., "Foam Generation in Porous Media," *Chem. Eng. Sci.*, **57**, pp. 4037-4052 (2002).
9. Kam, S.I. and Rossen, W.R. "A Model for Foam Generation in Homogeneous Porous Media," *paper SPE 77698, presented at the SPE ATCE, San Antonio, 29 Sept. - 2 Oct.* (2002).
10. Osterloh, W.T. and Jante, M.J. Jr. "Effects of Gas and Liquid Velocity on Steady-State Foam Flow at High Temperature," *paper SPE 24179 presented at the SPE/DOE Symposium on EOR, Tulsa, OK* (1992).
11. Alvarez, J.M., Rivas, H., and Rossen, W.R., "A Unified Model for Steady-State Foam Behavior at High and Low Foam Qualities," *SPEJ*, pp. 325-333 (Sept. 2001).
12. Mamun, C.K., Rong, J.G., Kam, S.I., Liljestrand, H.M., and Rossen, W.R., "Simulating Use of Foam in Aquifer Remediation," *Developments in Water Science*, **47**(1), pp. 867-874 (2002).
13. Kam, S.I., Frenier, W.W., Davies, S.N., and Rossen, W.R. "Experimental Study of High-Temperature Foam for Acid Diversion," *paper SPE 82266 presented at the SPE European Formation Damage Conference, The Hague, The Netherlands, 13-14 May* (2003).
14. Mamun, C.K., Rong, J.G., Kam, S.I., Liljestrand, H.M., and Rossen, W.R. "Extending Foam Technology from Improved Oil Recovery to Environmental Remediation," *paper SPE 77557 presented at the SPE ATCE, San Antonio, 29 Sept. - 2 Oct.* (2002).
15. Tanzil, D., Hirasaki, G.J., and Miller, C.A. "Conditions for Foam Generation in Homogeneous Porous Media," *paper SPE 75176 presented at the SPE/DOE Symposium on Improved Oil Recovery, Tulsa, OK, 13-17 April* (2002).
16. Khatib, Z.I., Hirasaki, G.J., and Falls, A.H., "Effects of Capillary Pressure on Coalescence and Phase Mobilities in Foams Flowing Through Porous Media," *SPERE*, pp. 919-926 (Aug. 1988).

17. Rossen, W.R. and Zhou, Z.H., "Modeling Foam Mobility at the Limiting Capillary Pressure," *SPE adv. Technol.*, **3**, p. 146 (1995).
18. Aronson, A.S., Bergeron, V., Fagan, M.E., and Radke, C.J., "The Influence of Disjoining Pressure on Foam Stability and Flow in Porous Media," *Colloids Surfaces A: Phisicochem. Eng. Aspects*, **83,** p. 109 (1994).
19. Bernard, G.G., Holm, L.W., and Jacobs, W.L., "Effect of Foam on Trapped Gas Saturation and on Permeability of Porous Media to Water," *SPE J.*, pp. 195-300 (Dec. 1965).
20. Sanchez, J.M. and Schechter, R.S., "Surfactant Effects on the Two-Phase Flow of Steam-Water and Nitrogen-Water Through Permeable Media," *J. Petr. Sci. Eng.*, **3**, pp. 185-199 (1989).
21. Cheng, L., Kam, S.I., Delshad, M., and Rossen, W.R., "Simulation of Dynamic Foam-Acid Diversion Processes," *SPEJ*, pp. 316-324 (Sept. 2002).
22. Rossen, W.R. and Wang, M.-W., "Modeling Foams for Matrix Acid Diversion," *SPEJ*, pp. 92-100 (June 1999).
23. Hirasaki, G.J. and Lawson, J.B., "Mechanisms of Foam Flow Through Porous Media Apparent Viscosity in Smooth Capillaries," *SPE J.*, pp. 175-190 (April 1985).
24. Collins, R.E., Flow of Fluids Through Porous Materials, Research & Engineering Consultants Inc., Eaglewood, CO (1961).
25. Alvarez, J.M., Rivas, H., and Navarro, G., An Optimal Foam Quality for Diversion in Matrix-Acidizing Projects, *paper SPE 58711 presented at the SPE International Symposium on Formation Damage Control, Lafayette, Louisiana, 23-24 Feb.* (2000).
26. Nguyen, Q.P., Currie, P.K., and Zitha P.L. "Effect of Capillary Cross-Flow on Foam-Induced Diversion in Layered Formations," *paper SPE 82270 presented at the SPE European Formation Damage Conference, The Hague, The Netherlands, 13-14 May* (2000).